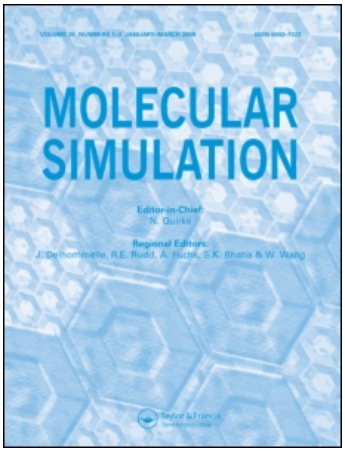

Molecular Simulation
Publication details, including instructions for authors and subscription information:
http://www.informaworld.com/smpp/title~content=t713644482

MD simulations of polymeric C_{60} fullerene layers/chain under tension

H. Shen[a]
[a] School of Aeronautics and Astronautics, Nanjing University of Aeronautics & Astronautics, Nanjing, People's Republic of China

To cite this Article Shen, H.(2006) 'MD simulations of polymeric C_{60} fullerene layers/chain under tension', Molecular Simulation, 32: 5, 385 — 390
To link to this Article: DOI: 10.1080/08927020600764998
URL: http://dx.doi.org/10.1080/08927020600764998

Molecular Simulation, Vol. 32, No. 5, 30 April 2006, 385–390

Taylor & Francis
Taylor & Francis Group

MD simulations of polymeric C_{60} fullerene layers/chain under tension

H. SHEN*

School of Aeronautics and Astronautics, Nanjing University of Aeronautics & Astronautics, Nanjing 210016, People's Republic of China

(Received January 2006; in final form March 2006)

The molecular dynamics (MD) method based on the Tersoff potential was used to simulate the tension and fracture of three polymeric $7 \times 7C_{60}$ fullerene layers, with no defect, one single-edge defect or one central defect, as well as one polymeric $7C_{60}$ fullerene chain. The effects of different type defect and tensile velocity on the fracture behavior and tensile mechanical properties of the C_{60} layers/chain were discussed and analyzed. It is shown that, (1) the C_{60} layers, with different type defect and different tensile velocity, have different cracking positions and fracture modes; (2) the fracture strength σ_c and deformation capability for the presented C_{60} layers/chain have the orders of "no-defect C_{60} layer > single-edge defect C_{60} layer > central defect C_{60} layer > $7C_{60}$ chain" and "no-defect C_{60} layer > single-edge defect C_{60} layer > $7C_{60}$ chain > central defect C_{60} layer", respectively; (3) the C_{60} layers/chain with high tensile-velocity have higher fracture strength σ_c, higher elastic module E but lower deformation capability than those with low velocity; (4) for the same tensile velocity the C_{60} layers have higher elastic module E than the C_{60} chain, and the no-defect C_{60} layer has the higher E than the two other C_{60} layers; (5) the C_{60} layers/chain have lower E but much higher tensile strength σ_c than steel.

Keywords: C_{60} layers/chain; Tensile properties; MD; Tensile velocity

1. Introduction

Carbon fullerene is a new form of carbon different from graphite and diamond. Due to its cage-like molecular configure, quantum size effect and geometric size effect, carbon fullerene shows unusual chemical, catalytic and photoelectric characters, and has extensive potential application in the fields of chemical industry, photoelectric materials and so on [1,2]. Since C_{60} fullerene, the best known and most stable fullerene, was first found by Kroto *et al*. [3], people have made much effort in preparing fullerene and investigating its micro-structure [2,4]. Interestingly, two kinds of C_{60} fullerene polymers, namely two-dimensional C_{60} layer [5] and one-dimensional C_{60} chain [6], were recently found at the high-pressure/high-temperature conditions. In the C_{60} polymers, the adjacent C_{60} fullerenes are bridged through a pair of parallel C–C bonds.

It is well known that nano-materials often have some peculiar properties. In order to fully utilize the nano-materials, firstly, people must thoroughly investigate their various physical and chemical characters. Now some studies on the polymeric C_{60} layer or C_{60} chain have been carried out. For example, the molecular or electronic structures of the C_{60} layer and C_{60} chain have been characterized through the spectroscopic techniques including X-ray, IR, Raman and so on [6,7–9]. However, the mechanical properties of the polymeric C_{60} layer or C_{60} chain have never been reported.

Considering the above reason, in the present paper the Tersoff potential based molecular dynamics (MD) method is used to simulate the tension of three square C_{60} single-layers and one $7C_{60}$ chain. At last the effects of different type defect and tensile velocity on their tensile properties are discussed further. Some conclusions in the present paper are very helpful for people to cognize the mechanical characters of the one-dimensional and two-dimensional C_{60} polymers.

2. The models and method

Figure 1 presents the investigated objects, three square $7 \times 7C_{60}$ single-layers and one $7C_{60}$ chain. Both the side-lengths L of the polymeric C_{60} layers and the length L of the $7C_{60}$ chain are about 6.84 nm. The C_{60} layer in figure 1(b)

*Tel: 86 025 8489202. Email: shj@nuaa.edu.cn

Molecular Simulation
ISSN 0892-7022 print/ISSN 1029-0435 online © 2006 Taylor & Francis
http://www.tandf.co.uk/journals
DOI: 10.1080/08927020600764998

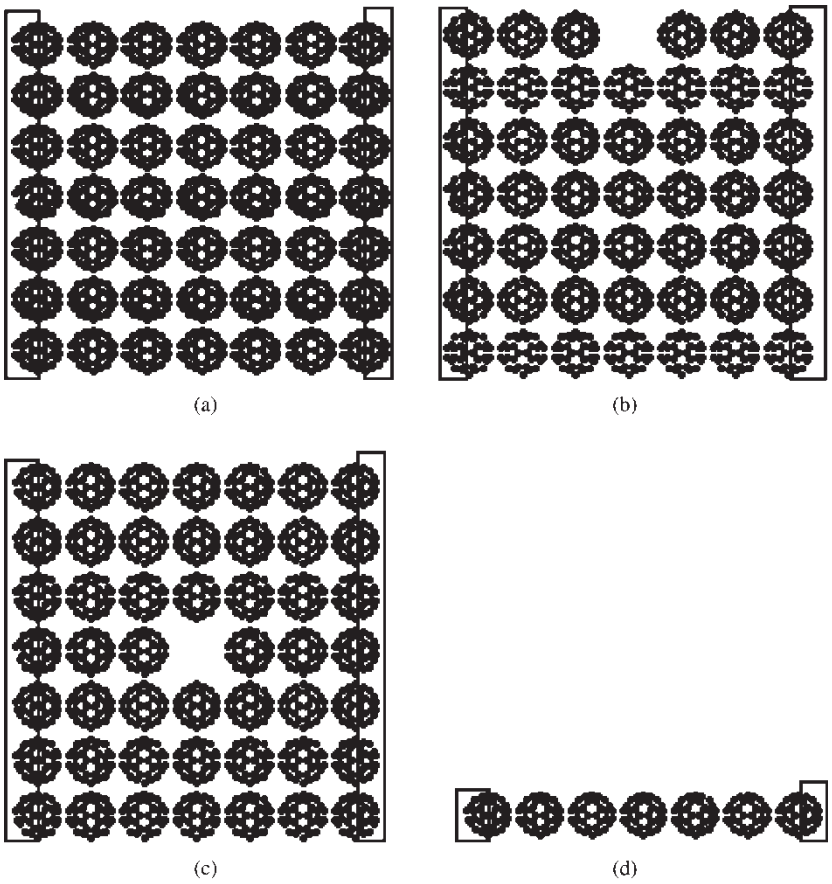

Figure 1. Polymeric C_{60} fullerene layers/chain. (a) no-defect C_{60} layer; (b) single-edge defect C_{60} layer; (c) central defect C_{60} layer; and (d) $7C_{60}$ chain.

has one single-edge defect and the one in figure 1(c) one central defect, considering the fact that the defects have been found in some polymeric C_{60} layer. Any two adjacent C_{60} fullerenes in these C_{60} polymers are bridged by two parallel C–C bonds and have the distance about 0.93 nm [6]. All the C_{60} fullerenes in the C_{60} layers/chain have the diameter of $D \approx 0.73$ nm.

Both the molecular modeling and geometry optimization of the C_{60} layers/chain in figure 1 are performed in the famous quantum-chemical software of HyperChem 7 [10]. In the geometry optimization, the MM+ force field and the Fletcher's conjugate gradient method [11] are adopted, and the energy convergence limit takes 0.01 Kcal/mol.

In the present paper the classical MD method is used to simulate the tension of the C_{60} layers/chain. During the simulations the carbon atoms in the left frames of figure 1 are fixed, and the atoms in the right frames are tensioned horizontally. The tensile velocity v takes 0.06, 0.09 or 0.12 nm/ps, i.e. the displacement of 0.06, 0.09 or 0.12 nm is applied per 1000 time-steps. Among the empirical model potentials that have been developed for carbon molecular-systems, the Tersoff potential [12,13], based on the concept of bond order, is recognized to be the most successful one. Recently the second-generation Brenner potential [14] improves analytic function for the intramolecular interaction which results in a significantly better description of bond length, energy and force constant. However, in many works about carbon system [15], the Tersoff potential is still used. In this paper we use the Tersoff potential to describe the interaction of the bonded carbon atoms. For two neighbouring carbon atoms i and j, the Tersoff form of the energy Φ is taken to be [12,13]

$$\Phi = \sum_i \sum_{j>i} f_c(r_{ij})[E_r(r_{ij}) - b_{ij}E_a(r_{ij})] \tag{1}$$

with

$$E_r(r_{ij}) = A\exp(-\lambda r_{ij}) \qquad E_a(r_{ij}) = B\exp(-\mu r_{ij}) \tag{2}$$

$$f_c(r_{ij}) = \begin{cases} 1 & r_{ij} < R \\ \frac{1}{2}\left[1 + \cos\left(\pi\frac{r_{ij}-R}{S-R}\right)\right] & R < r_{ij} < S \\ 0 & S < r_{ij} \end{cases}$$

b_{ij} is the many-body order parameter describing how the bond-formation energy is affected by the local atomic arrangement due to the presence of other neighbouring atoms (the k-atoms). It is a many-body function of the positions of the atoms i, j and k. It has the form of

$$b_{ij} = \chi\left(1 + \beta^n \xi_{ij}^n\right)^{-\frac{m}{2n}} \tag{3}$$

with

$$\xi_{ij} = \sum_{k \neq i,j} f_c(r_{ik}) \omega g(\theta_{ijk}) \tag{4}$$

$$g(\theta_{ijk}) = 1 + \frac{c^2}{d^2} - \frac{c^2}{d^2 + (h + \cos\theta_{ijk})^2}$$

where, r_{ij} is the distance of the ith and jth atom, θ_{ijk} is the angle between r_{ij} and r_{jk}, $f_c(r_{ij})$ is a truncation function. A, B, λ, μ, χ, β, n, m, ω, c, d, h, R and S are some correlative constants with the i-j-k atomic system, and their values take the corresponding ones in Ref. [12] and [13].

Considering the fact that the interaction of the unbonded carbon atoms is comparatively small the unbonded interaction is ignored in the simulations. The time step Δt takes 0.001 ps, and the temperature 300 K. The ensemble takes the NTV one, and the velocity the Verlet's expression [16].

3. Results and discussion

3.1 The fracture modes

Figure 2 (a)–(d) presents the fracture modes of the presented C_{60} layers/chain with $v = 0.06$ and 0.12 nm/ps. In figure 2 the arrows are used to mark the start positions and propagation paths of the cracks, and the numbers of "1" and "2" indicate the cracking sequence of the cracks. The fracture modes of the C_{60} layers/chain with $v = 0.09$ nm/ps is very similar to the cases of $v = 0.06$ nm/ps, and are not given here.

According to figure 2, it can be found that:

(1) The C_{60} layers (or C_{60} chain) crack between two row (or two) C_{60} fullerenes, and the cracks are perpendicular to the tensile direction. After fracture, all the C_{60} fullerenes in the C_{60} layers/chain have little change in structure.
(2) The C_{60} fullerenes in the C_{60} polymers are elongated in the tensile direction and are shortened perpendicular to the tensile direction during the tension, namely the C_{60} fullerenes become ellipsoids during the tension.
(3) The C_{60} layers (or C_{60} chain) with different tensile velocity have obviously different fracture modes. Namely, the no-defect C_{60} layer with $v = 0.06$ and 0.12 nm/ps cracks between the two row C_{60} fullerenes most close to the loading end, but, for the case of $v = 0.06$ nm/ps, another incidental crack still appears between the second and third row fullerenes, see figure 2 (a); the single-edge defect C_{60} layer with $v = 0.06$ and 0.12 nm/ps does not crack from the defect, instead between the second and third row fullerenes, but, for the case of $v = 0.06$ nm/ps, the start position of crack is close to the center of the C_{60} layer, and for $v = 0.12$ nm/ps the start position lies at the side with no defect, see figure 2 (b); the central defect C_{60} layer with $v = 0.06$ and 0.12 nm/ps cracks from the central defect, but the start position of crack is still slightly different, see figure 2 (c); the C_{60} chain with $v = 0.06$ nm/ps fractures between the second and third C_{60} fullerene close to the loading end, but, for the case of $v = 0.12$ nm/ps, the C_{60} chain fractures between the first and second C_{60} fullerene, see figure 2 (d).
(4) The single-edge defect C_{60} layer does not crack, but the central defect C_{60} layer from its defect, which implies that the cracking of the C_{60} layers is more sensitive to the central defect. So it is predictable that, of the presented C_{60} layers, the central defect one will have the worst mechanical properties.

3.2 The tensile curves

Figure 3 shows the stress-strain curves (σ–ε curves) of the C_{60} layers/chain with $v = 0.06$,0.09 and 0.12 nm/ps. Here the tensile-stress σ is defined as $\sigma = F/S$, in which F is the external loading, and S is the tensile area. For the C_{60} layers $S = D \times L$, and for the C_{60} chain $S = D^2$. The tensile strain ε is defined as $\varepsilon = \Delta L/L$, in which ΔL is the tensile displacement. In figure 3 the arrows $\leftarrow$ mark the moment of the C_{60} layers/chain cracking.

From figure 3, it is shown that:

(1) With the tensile strain ε increasing, the stress σ for the C_{60} layers/chain increases zigzagedly, reaches the maximum σ_c at the positions marked by "$\leftarrow$", and then decreases quickly until the C_{60} layers/chain fail, where the maximal stress σ_c is called as fracture stress and the corresponding strain ε_c are defined as the failure strain.
(2) Within the range of $\varepsilon < \varepsilon_c$, for the same strain ε, all the three C_{60} layers have larger stress than the $7C_{60}$ chain, and the no-defect C_{60} layer has slightly larger stress than two other C_{60} layers. The phenomenon can be explained as followings: Firstly, in the C_{60} layers there are lots of C–C bonds that are perpendicular to the tensile direction and between the C_{60} fullerenes, during the tension the C–C bonds are tensioned and hinder the shrinkage of C_{60} fullerenes perpendicular to the tensile direction, so, for the same tensile strain ε, the three C_{60} layers have larger tensile-stress σ than the $7C_{60}$ chain; secondly, the single-edge and central defects reduce the load support capability of the C_{60} layer, so, for the same tensile strain ε, the no-defect C_{60} layer has larger stress than the single-edge and central defect C_{60} layers.
(3) The fracture stress σ_c and the fracture strain ε_c are often used to characterize the fracture strength and the deformation capability of materials respectively. Generally, the larger the σ_c and ε_c are, the higher the fracture strength and the deformation capability of materials are. According to figure 3, apparently the fracture strength of the C_{60} polymers has the order of "no-defect C_{60} layer > single-edge defect C_{60} layer > central defect C_{60} layer > $7C_{60}$ chain", and the fracture strain, namely the deformation

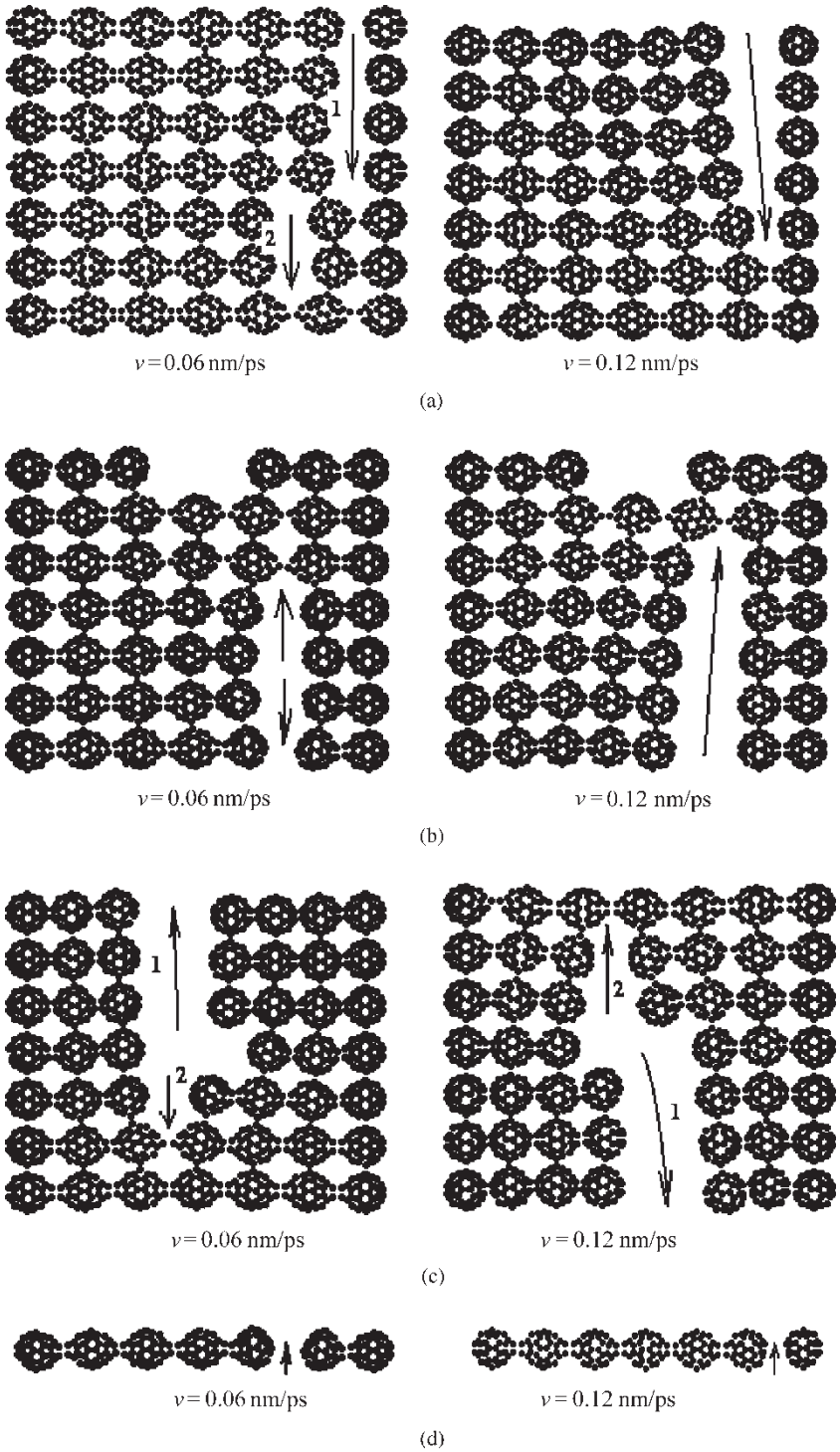

Figure 2. Tensile fracture of the C_{60} layers/chain. (a) no-defect C_{60} layer; (b) single-edge defect C_{60} layer; (c) central defect C_{60} layer; and (d) $7C_{60}$ chain.

capability, has the order of "no-defect C_{60} layer > single-edge defect C_{60} layer > $7C_{60}$ chain > central defect C_{60} layer".

3.3 The effects of tensile velocity on tensile properties

Figure 4 presents the $\sigma-\varepsilon$ curves of the C_{60} layers/chain with different tensile velocity. According to figure 4, it is found that the $\sigma-\varepsilon$ curves the C_{60} layers/chain under different tensile velocity are distinctly different. Firstly, the C_{60} layer/chain with low tensile-velocity has much smaller fracture strength σ_c but much higher fracture strain ε_c than that with high velocity. Secondly, for the same strain, the stress of the C_{60} layer/chain with high tensile-velocity is obviously larger than that with low velocity.

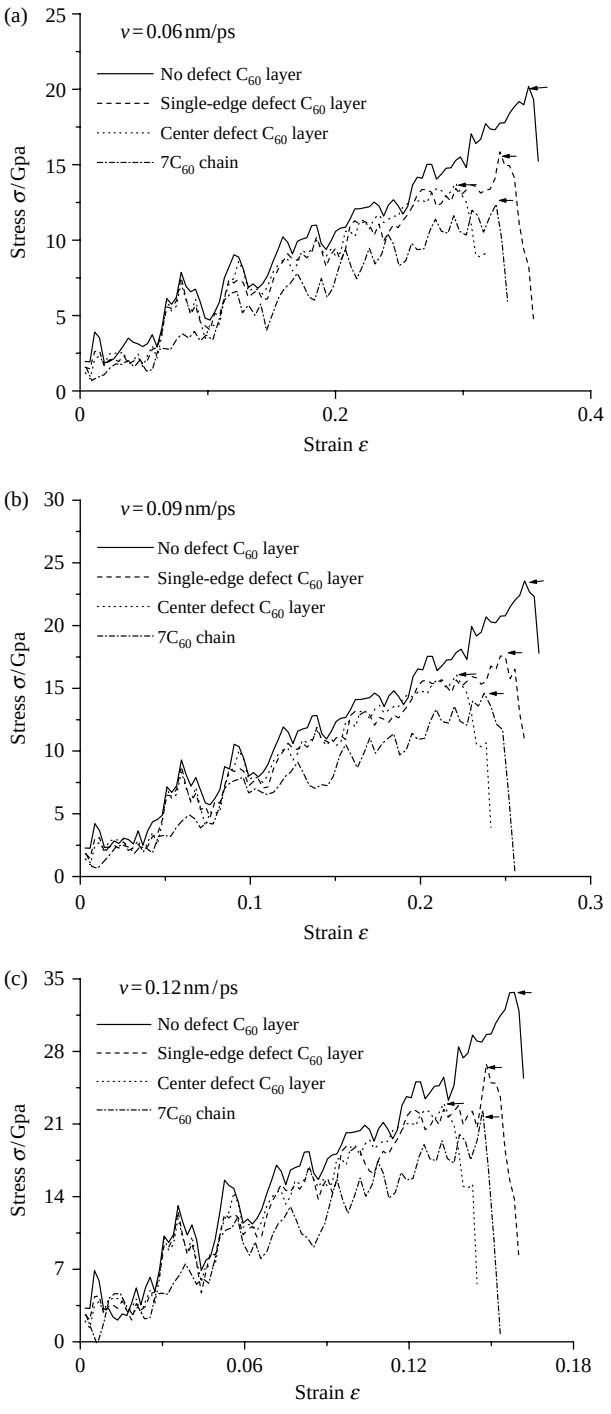

Figure 3. The σ–ε curves of the C_{60} layers/chain with (a) $v = 0.06$; (b) $v = 0.09$; and (c) $v = 0.12$ nm/ps.

Table 1 lists the fracture strength σ_c, fracture strain ε_c and elastic module E for all the C_{60} layers/chain with $v = 0.06$, 0.09 and 0.12 nm/ps. Here the elastic module E is estimated according to the following method: linearly fitting all the σ–ε curves for $\sigma < \sigma_c$ in the famous data-processing software of Origin 6, and approximatively regarding the slope of the fitted lines as the corresponding E.

Table 1 indicates that: (1) the elastic module E of all the C_{60} layers/chain with high tensile velocity is larger than

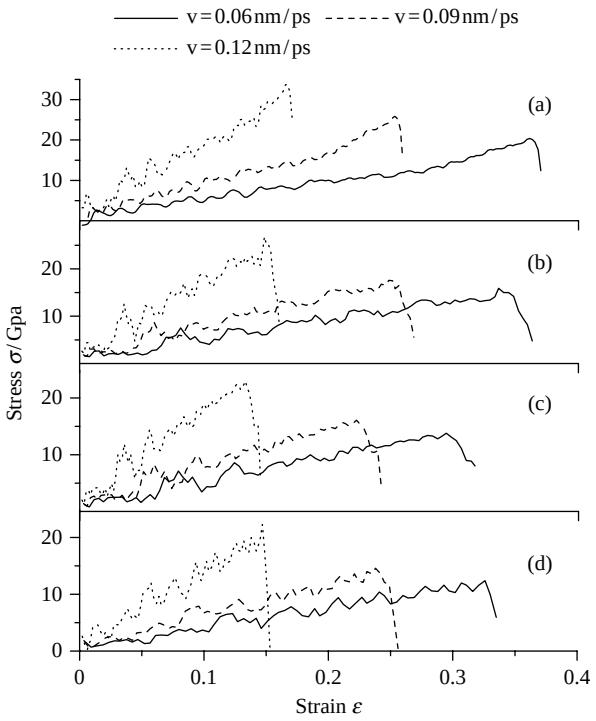

Figure 4. The σ–ε curves of (a) the no-defect C_{60} layer; (b) the single edge-defect C_{60} layer; (c) the central defect C_{60} layer; and (d) the $7C_{60}$ chain under different tensile velocity.

the ones with low velocity; (2) for the same tensile velocity the C_{60} layers have higher E than the C_{60} chain and the no-defect C_{60} layer has the higher E than the other C_{60} layers; (3) all the C_{60} layers/chain with $v = 0.06$,0.09 or 0.12 nm/ps have the fracture strain ε_c of 13.4 $\sim$ 35.9%, the fracture strength σ_c of 12.3 $\sim$ 34.0 Gpa and the elastic module E of 37.8 $\sim$ 209.8 Gpa. The fracture strain ε_c is comparable to that of steel, 25 $\sim$ 55%, the elastic module E is lower than that of steel, 200 Gpa; but the fracture strength σ_c is much higher than that of steel, 0.25 $\sim$ 0.33 Gpa. Here all the ε_c, E and σ_c data for steel come from reference [17]. This implies that the C_{60} layers/chain in the present paper are a kind super-high-strength material.

Table 1. Fracture strength σ_c, fracture strain ε_c and elastic module E for C_{60} layers/chain.

Tensile velocity v/nm/ps	*C_{60} polymer*	*σ_c/Gpa*	*ε_c/%*	*E/Gpa*
0.06	No defect layers	20.3	35.9	56.5
	Single-edge defect layer	15.7	33.3	47.1
	Center defect layer	13.6	29.2	46.6
	$7C_{60}$ chain	12.3	32.5	37.8
0.09	No defect layers	25.2	26.1	96.6
	Single-edge defect layer	17.9	24.8	72.2
	Center defect layer	16.6	22.5	73.8
	$7C_{60}$ chain	14.9	23.8	62.6
0.12	No defect layers	34.0	16.1	209.8
	Single-edge defect layer	26.7	14.8	180.4
	Center defect layer	24.9	13.4	185.8
	$7C_{60}$ chain	21.6	14.7	146.9

4. Conclusions

The Tersoff potential based MD simulations were performed to analyze the tensile fracture of three polymeric C_{60} fullerene layers, with no defect, single-edge defect or central defect, and one polymeric $7C_{60}$ fullerene chain. The effects of different type defect and tensile velocity on the tensile mechanical properties of the C_{60} layers/chain were compared and discussed. The results are concluded as follows:

(1) The C_{60} layers, with different type defect and tensile velocity, have different fracture modes.
(2) The fracture strength for the presented C_{60} layers/chain conforms to the order of "no-defect C_{60} layer $>$ single-edge defect C_{60} layer $>$ central defect C_{60} layer $>$ $7C_{60}$ chain", and the deformation capability the order of "no-defect C_{60} layer $>$ single-edge defect C_{60} layer $>$ $7C_{60}$ chain $>$ central defect C_{60} layer".
(3) The C_{60} layers/chain with high tensile-velocity have higher fracture strength, higher elastic module but lower deformation capability than those with low velocity. For the same tensile velocity the C_{60} layers have higher E than the C_{60} chain, and the no-defect C_{60} layer has the higher E than the two other C_{60} layers.
(4) The C_{60} layers/chain have much higher tensile strength but lower elastic module than steel.

References

[1] N.S. Saricftci, L. Smilowitz, *et al.* Photo-induced electron transfer from conduction polymers onto buckminister-fullerene. *Science*, **258**, 1474 (1992).
[2] R.E. Smalley. Self-assembly of fullerenes. *Acc. Chem. Res.*, **25**(2), 98 (1992).
[3] H.W. Kroto, J.R. Heath, S.C. Brien, R.F. Curl, R.E. Smalley. C_{60}: buckminsterfullerene. *Nature*, **318**, 162 (1985).
[4] J.R. Heath. Synthesis of C_{60} from small carbon clusters, a model based on experiment and theory. *ACS. Symp. Ser.*, **481**(1), 1 (1991).
[5] R. Moret, P. Launois, T. Wagberg, B. Sundqvist. High-pressure synthesis, structural and Raman studies of a two-dimensional polymer crystal of C_{60}. *Eur. Phys. J. B*, **15**, 253 (2000).
[6] S. Pekker, G. Oszlanyi, L. Forro. Polymeric fullerene chains in RbC_{60} and KC_{60}. *Nature*, **370**, 636 (1994).
[7] A. Talyzin, L. Dubrovinsky, M. Oden, T. Le Bihan, U. Jansson. *Insitu* X-ray diffraction study of C_{60} polymerization at high pressure and temperature. *Phys. Rev. B*, **66**, 165409 (2002).
[8] V.V. Belavina, L.G. Bulushevab, A.V. Okotrubb, D. Tomanekc. Stability, electronic structure and reactivity of the polymerized fullerite forms. *J. Phys. Chem. Sol.*, **61**, 1901 (2000).
[9] A.M. Rao, P.C. Eklund, J.L. Hodeau, L. Marques, M. Nunez-Regueiro. Infrared and raman studies of pressure- polymerized C_{60}. *Phys. Rev. B*, **55**, 4766 (1997).
[10] Hypercube Inc. *Users' Manual of Hyperchem Realse 7*, Hypercube Inc., Gainesville (2002).
[11] R. Fletcher, C. Reeves. Function minimization by conjugate gradients. *Comput. J.*, **7**, 149 (1964).
[12] J. Tersoff. New empirical model for the structural properties of silicon. *Phys. Rev. Lett.*, **56**(6), 632 (1986).
[13] J. Tersoff. Empirical interatomic potential for carbon, with applications to amorphous carbon. *Phys. Rev. Lett.*, **61**(25), 2879 (1988).
[14] D.W. Brenner, O.A. Shenderova1, J.A. Harrison, S.J. Stuart, B. Ni, S.B. Sinnott. A second-generation reactive empirical bond order (REBO) potential energy expression for hydrocarbons. *J. Phys. Condens. Matter*, **14**, 783 (2002).
[15] J.G. Chang, C.C. Hwang, S.P. Ju, S.H. Huang. A molecular dynamics simulation investigation into the structure of fullerene C_{60} grown on a diamond substrate. *Carbon*, **42**, 2609 (2004).
[16] A.R. Leach. *Molecular Modeling*, Addison Wesley Longman Limited, England (1996).
[17] F. Yue. *Engineering Material*, p. 11, The BUAA Press, Peking (2003).